Short-term observation of electric ablation with nanosecond pulsed electric field in the hepatic hilar area

Jiahua Lu
Zhejiang University
Junjie Qian
Zhejiang University School of Medicine First Affiliated Hospital
Shiyu Zhang
Zhejiang University School of Medicine First Affiliated Hospital
Xinhua Chen
Zhejiang University School of Medicine First Affiliated Hospital
Shengyong Yin
Zhejiang University School of Medicine First Affiliated Hospital
Lin Zhou
Zhejiang University School of Medicine First Affiliated Hospital
Shusen Zheng
Zhejiang University School of Medicine First Affiliated Hospital
Wu Zhang (zhangwu516@zju.edu.cn)

Research

Keywords: Nanosecond pulsed electric field (nsPEF), Hepatocellular carcinoma (HCC), Tumor ablation, Liver vasculature, Hepatic hilar area.

Posted Date: April 15th, 2020

DOI: https://doi.org/10.21203/rs.2.23523/v2

Abstract

Background: Treatment of liver malignancies located in the hepatic hilar area has long been recognized as a challenge for both surgeons and interventional radiologists. Traditional locoregional thermal ablative therapies such as radiofrequency ablation (RFA) turned to fail in achieving complete ablation near the major vasculatures. **The** nanosecond pulsed electric field (nsPEF) has emerged as a novel electric power-based locoregional therapy. It has been reported to effectively ablate liver malignancies without causing obvious damage. This preclinical study was conducted on animal models to evaluate the safety and feasibility of nsPEF ablation in the hepatic hilar area and to investigate its long-term effect on liver vasculature systems.

Methods: Two nsPEF needle electrodes were placed around the hepatic hilar areas in the rabbit liver with ultrasonic guidance. During and after nsPEF ablation, electrocardiography (ECG) was used to monitor cardiovascular activity, and ultrasonography was used to detect blood flow changes. Blood samples and liver specimens were collected pre-treatment and 2 hours, 2 days, 7 days, 14 days and 28 days posttreatment.

Results: Histopathological studies showed that the liver tissues in the targeted portal area were ablated accurately without perivascular sparing. The major structures of the large hepatic veins and bile ducts near hilar areas were preserved well. Follow-up biochemical tests showed a transient impairment of liver function. The results of myocardial enzymes and blood routine proved that nsPEF will not cause collateral damage to cardiac systems or increase potential infection risks. Ultrasonography and electrocardiography found no massive hemorrhea or abnormal cardiac activities.

Conclusion: Our results demonstrate that nsPEF is highly effective and feasible for the ablation of liver tissues in the hepatic hilar area. During the treatment, nsPEF did not disturb vital organ functions or cause irreversible complications, proving its safety. Furthermore, nsPEF can ablate the hepatic hilar area without damaging large hepatic vasculatures, which could be a promising method for nonthermal tumor ablation.

Background

Liver cancer is the sixth most commonly diagnosed cancer and the fourth leading cause of cancer-related death worldwide [1]. According to the latest guidelines, surgery is still the most important and effective approach to achieve long-term survival for liver cancer patients . However, some patients are already in an advanced stage when first diagnosed and therefore do not have the opportunity for surgery. These patients have to resort to locoregional therapies such as thermal ablation or transarterial chemotherapy to avoid invasive damage.

Thermal ablation is commonly used to treat the patients with poor liver function or a tumor size less than 3 cm. However, traditional thermal ablation methods such as radiofrequency (RFA) and microwave ablations (MWA) face major challenges during the treatment of liver tumors adjacent to large vessels.

First, flowing blood in the large vessels removes thermal energy during the ablation, which may lead to incomplete ablation of tumor tissues, known as the “heat-sink” effect [3-6]. Second, overheating causes damage to blood vessels and bile ducts, which may lead to serious complications [7-9].

Benefitting from updated pulsed power technology, a new electric locoregional ablation technique known as the nanosecond pulsed electric field (nsPEF) has emerged in cancer treatment. NsPEF is characterized by an ultrashort pulse duration (nanosecond) and extremely high electric field intensity (higher than 10 kv/cm), which enables the electric current to break through tumor tissues and achieve complete ablation [10-12]. At the cellular level, nsPEF penetrates the cellular membrane with high electric energy and produces irreversible nanopores, which leads to apoptosis of cancer cells [13, 14]. Furthermore, nsPEF enhances tumor antigen presentation of dendritic cells (DCs) and thus promotes an adaptive immune response against tumor [15]. In recent clinical trials, nsPEF also demonstrated encouraging therapeutic effects in human basal cell carcinoma (BCC) with little scarring and reduced pain in patients [16].

Unlike conventional thermal ablative therapies, nsPEF ablates the tumor tissues based on high-intensity electric power instead of thermal energy (70-95°C) [17]. This nonthermal characteristic of electric ablation theoretically enables it to be unaffected by so-called “heat-sink” effects. In addition, it should not cause uncontrolled thermal damage to vasculature systems. Considering the above features, we speculated that nsPEF could be identified as the first option for locoregional ablation of the liver malignancies located around the large vessels or bile ducts, especially those in the hepatic hilar area. Therefore, we performed experiments to verify the safety, feasibility and efficacy of nsPEF ablation in the hepatic hilar areas on in nontumor-bearing rabbit models.

We demonstrated for the first time that the standard nsPEF treatment with strict control of the parameters could achieve uniform ablation in hepatic hilar areas without obvious side effects in large animals. Furthermore, the structure of large hepatic vasculatures including blood vessels and bile ducts, in the ablation area was preserved well under nsPEF treatment, which proved its feasibility in the ablation of tumors in high-risk areas in the liver.

Results

NsPEF treatment will not influence the blood flow of the large vessels

The real time ultrasound monitoring of one rabbit during the treatment is shown in Fig.1. The distance between the two needles was approximately 10.5 mm (Fig.1a). No massive hemorrhage was found in the ablation area after electrode puncture (Fig. 1b). There was a hypoechoic area revealed by ultrasonography 15 minutes posttreatment consistent with the ablation region defined by pathology stain (Fig. 1c). The color ultrasonic flow imaging showed a mild local circulation deficiency in the hepatic hilar area, and no thrombosis formation or massive circulation deficiency was found 15 minutes after ablation (Fig. 1d).

NsPEF could achieve complete tissue ablation and preserve the structure of large vessels

Figure 2 shows the gross anatomy of the liver specimens, including newly harvested tissues (Fig. 2a – 2e) and according formalin fixed tissues (Fig. 2f – 2j). Changes in the ablated area were identified at different time points, including congestion or swelling (Fig. 2f – 2g) – inflammation (Fig. 2g) – recovery (Fig. 2h) – fibrosis (Fig. 2i) and dissolution (Fig. 2j). A distinct border line between the ablation area and normal tissue appeared 14 days post-treatment (Fig. 2i). Figure 3 shows the pathologic changes in the ablated area. Extensive red blood cells infiltrates into the sinusoids in the ablation zone 2 hours posttreatment. Endothelial damage was hardly observed in the large blood vessels immediately after ablation, and the bile ducts were almost intact. On day 2, parts of the endothelial layers of the large veins had shed, but they maintained a complete structure. Massive numbers of inflammatory cells had infiltrated into the ablated area. Some minor vessels were completely destroyed, leaving the rough contour lines. The bile ducts in the ablated area showed mild inflammatory changes. Reendothelialization in the vessels occurred 7 days posttreatment, and the large veins maintained their complete structure. By 14 days posttreatment, vascular congestion and infiltration of inflammatory cells had resolved in the ablated zone. Neovascularization appeared around the large vessels and in the margin of the ablated area. At 28 days posttreatment, the dead cells in the ablated zone were completely replaced by regenerated hepatocytes and fiber matrix.

NsPEF ablation slightly affect liver function

Figure 4 shows the changes in liver function during nsPEF treatment. The tested parametres included total protein (TP), albumin (Alb), globulin (Glb), alanine aminotransferase (ALT), aspartate aminotransferase (AST), alkaline phosphatase (ALP), total bilirubin (TB), direct bilirubin (DB), and total bile acid (TBA). ALT and AST rose transiently from 2 hours to 2 days posttreatment, while TP and Alb demonstrated no obvious changes, indicating that liver function underwent transient damage. There were no obvious changes in serum bilirubin (TB and DB), which suggests that nsPEF did not cause side effects on biliary systems. TBA showed a slight change after ablation and immediately returned to normal levels. ALP and Glb remained steady during the whole procedure. These results indicated that the damage caused by nsPEF to the hepatic and biliary systems can be repaired and compensated by the remaining normal liver tissues.

NsPEF ablation will not cause myocardial injury

Figure 5 shows that levels of myocardial enzymes, including heart type creatine kinase (CK), creatine kinase isoenzyme (CK-MB), lactate dehydrogenase (LDH), and hydroxybutyrate dehydrogenase (HBDH), increased rapidly after the ablation and returned to normal levels at 2 days posttreatment. Meanwhile, the level of cardiac troponin I (cTnI) remained under 0.01 ng/ml before, during and after the whole procedure (Additional File 1: Table S1). These results showed transient damage to skeletal muscles and hepatocytes instead of myocardial systems, which was caused by electrode puncture. And this damage was repairable and tolerable.

Peripheral blood tests showed no signs of infection after nsPEF ablation

Figure 6 shows the changes in routine blood test results, including the red blood cell count (RBC), white blood cell count (WBC), neutrophilic granulocyte percentage (NEUT), hemoglobin (Hgb), hematocrit (HCT), blood platelet count (PLT), mean corpuscular hemoglobin (MCH), and mean corpuscular hemoglobin concentration (MCHC), and mean corpuscular volume (MCV). There were no significant changes in the above results in the treated group compared with those in the untreated groups except for PLT. Hgb and the RBC remained steady the whole procedure, indicating no massive hemorrhage. NEUT demonstrated no significant changes, which ruled out the nsPEF treatment-related infections. PLT rose from 2 days to 7 days posttreatment, suggesting the potential procoagulant state of the peripheral blood.

Discussion

The nanosecond pulsed electric field is an emerging locoregional electric ablative therapy that can be used to treat a variety of solid tumors, including melanoma [17], breast cancer [18], colon cancer [11], osteosarcoma [19], pancreatic cancer [20] and hepatocellular carcinoma [21]. The nonthermal characteristic and avoidance of heatsink effects are two of the most significant features of nsPEF ablation, which makes it possible to apply nsPEF ablation on liver tumors located near vital structures such as the porta hepatis. Operation in this area is recognized as complicated for surgeons and is considered as a relative contraindications for RFA [22, 23].

In this study, we demonstrated for the first time that nsPEF achieved complete ablation of liver tissues and preserved the large vessels within ablation areas well. Conventional thermal ablations such as RFA relies on excessive heat energy to cause necrosis of liver tissues. They cannot discriminate parenchymal hepatic tissues from matrix tissue, such as vascular fibers, which may lead to vascular damages [24]. However, nsPEF uses electric pulses to generate irreversible nanopores on the cell membrane and does not damage other types of molecules, which explains why it has the potential to preserve the cellular matrix of the large vessels. As the short-term and mid-term pathological follow-up shows, the large vessels, including veins and bile ducts, in the ablated area maintained a complete vascular structure and the perivascular tissues were ablated accurately with no sparing. It was confirmed that the large vessels were protected from electric damage. Although some of the large vessels exhibited mild muscularis layer damage and endothelial loss, the presence of the extracellular matrix greatly facilitated the reendothelialization process within 14 days. This may also contributes to the significant immune responses and rapid tissue healing observed in a series of nsPEF treatment studies [16, 18, 21, 25]. Another interesting phenomenon is that compared with veins, bile ducts maintained a more complete structure, and the biliary epithelial cells were better preserved. According to previous studies about RFA, it is assumed that bile ducts are more vulnerable to thermal damage and less vulnerable to electric stimulations [9, 26, 27].

The protective effects on vasculature systems, especially for bile ducts, were also validated by the blood test results. Serum bilirubin, including TB and DB, showed no obvious changes during the whole procedure, indicating that nsPEF treatment did not cause biliary complications. However, biliary complications, such as cholestasis secondary to bile duct strictures that resulted from the thermal

damage, was of high incidence after RFA [28]. In addition, TBA underwent mild changes immediately after the treatment but then remained steady, suggesting that nsPEF may slightly disturb lipid metabolism. Notably, the number of blood platelets (PLT) increased posttreatment , which raises the concern of thrombosis formation. Although the thrombosis was not found in the histopathologic results, and the PLT went down at 14 days posttreatment, the increasing trend of PLT indicated a procoagulant effect of nsPEF. Previous studies reported that thrombogenicity is one of the risk factors after thermal ablation, and can lead to the administration of heparin [29]. For the above reasons, coagulation function of the patients should be monitored after nsPEF treatment.

Aminotransferases (ALT and AST) underwent a temporary increase, which was assumed to be resulted from hepatic parenchymal cells death. Their subsequent recovery confirmed the safety of nsPEF. Additionally, TP and Alb proved that nsPEF does not impair the capacity of albumin synthesis in the liver. According to the routine blood tests, RBC and Hb remained at the same level, proving that no massive hemorrhage occurred during the treatment. Furthermore, the results for inflammation, such as the percentages of neutrophils, did not change significantly, which indicated that strict asepsis during the operation could effectively avoid the risks of infection during the ultrasound-guided puncture process.

The effect of the electric ablation on the cardiovascular and skeletal muscle systems was investigated in this study. Previous studies proved that the release of high voltage energy increases cell membrane permeability and opens a path for ion transport, which can induce cardiac arrythmias and defibrillation, and may lead to unpredictable cardiac complications [30-32]. In addition, the electric stimulation of excitable tissues, such as motor nerves can cause involuntary contraction of the muscles of subjects, which may hinder the treatment [33-35]. However, in this study, we adopted the synchronization pulse generating system, which would automatically stop if the ECG detected abnormal heart activities, effectively protecting cardiovascular muscles from electric damage. The slight increase in the myocardial enzymes CK and CK-MB was caused by muscle puncture rather than myocardial injury, and the results for Cardiac troponin I confirmed this assumption. CK-MB-related muscle damage and mild increases in LDH and HBDH are tolerable in liver cancer patients. In addition, the use of the general anesthesia and insulated electrode needles prevented the contraction of skeletal muscles. These results proved that the appropriate operation of the synchronization pulse generating system and general anesthesia in nsPEF treatment is necessary.

However, certain problems remain to be solved in the future experiments. (1) It is difficult to find the accompanying arteries of the large veins in the hepatic hilar area under ultrasound guidance and even harder to include the three kinds of vessels (hepatic veins, arteries and bile ducts) in the ablation zone at one time. Therefore, our research mainly focused on the effect of nsPEF ablation on large hepatic veins and bile ducts and some of the minor arteries. However, the effect of nsPEF on large arteries requires further investigation. (2) The risk of thrombosis formation, as reflected by PLT, should be evaluated in the long-term follow-up studies. Such evaluation requires not only the reexamination of coagulation functions, but also the regular ultrasonic monitoring of the large vascular.

Conclusion

Overall, nsPEF is safe and feasible for the ablation of tissues in the hepatic hilar area and the minimally invasive characteristic of this electric ablation method may expand its application in end-stage, HCC patients with poor liver functions. Furthermore, nsPEF has a potential protective effect on hepatic vasculature systems, which serves as support for its use to ablate liver malignancies located near the porta hepatis. It is one of the newest techniques available for treating hard-to-reach tumors by offering another option for patients who have tumors that are close to blood vessels, ducts or nerves that may otherwise be damaged by heat-based ablation techniques, such as RFA, MWA and cryotherapy. Multiple center clinical trial investigations (Clinical trial #NCT04309747 “A prospective multicenter clinical trial of safety and effectiveness of Nanosecond knife ablation for liver cancer ”) are ongoing to verify the clinical outcomes of nsPEF in patients.

Material And Methods

Animals and anesthesia

This study was approved by the Animal Care and Use Committee of the Zhejiang Academy of Medical Sciences. The anesthesia and treatment procedure were fully complied with the animal experimental guidelines. All animals received appropriate humane care from certificated professional staff. A total of 20 New Zealand White rabbits (2.2 kg ± 0.2 kg) were purchased and maintained by the Division of the Experimental Animal Laboratory of Zhejiang Academy of Medical Sciences. General anesthesia was maintained with 1.5% - 2% isoflurane by mechanical ventilation during the procedure (Fig. 8c). The basic vital signs of each rabbit were monitored using an ECG machine and observed and documented by an experienced anesthetist (Fig. 8). Vital signs were stable during and after the whole treatment procedure. ECG did not detect severe heart arrhythmia or other abnormal cardiac activities. Minor complications, including subcutaneous hematoma and pneumothorax, were not found during and after the nsPEF treatment.

Nanosecond pulsed electric field treatment

All the nsPEF treatment procedures were performed via open laparotomy and the abdomen was closed after the ablation treatment (Fig. 8a). The pulse generator device was provided by Ready Biological Technology LTD (Hangzhou, Zhejiang, China) and had two electrode needles (Fig. 8d). The effective tip length to generate an electric field is 2 cm (Fig.8b). The nsPEF treatment parameters were set as follows: each pulse duration was 300 ns, 800 pulses were conducted in each treatment, the pulse frequency was 2 Hz, and the electric field intensity was maintained at 25000 V/cm. The real time monitoring of tissue impedance and electric current were recorded and documented in Table 1. Electrocardiograph was used to monitor the cardiac activities and to ensure that the pulses were generated during the absolute myocardial refractory period to prevent heart arrhythmias. The parameters were set and adjusted according to our previous ablation experience in rabbits with liver cancer.

Ultrasound guidance and evaluation

Before treatment, ultrasonography was used to identify the hepatic hilar area and guide the needle puncture (Fig. 8c). Fifteen minutes after the ablation, the width and length of the ablated area were measured by ultrasonography (Mylab Gamma, Esaote Group, Italy). Blood perfusion in and around the ablated area was monitored. All ultrasound procedures were performed by an experienced ultrasonic operator.

Blood biochemical follow-up

Blood samples were collected at 2 hours before nsPEF treatment and at 2 hours, 2 days, 7 days, 14 days, and 28 days posttreatment in order to dynamically observe the changes in liver function, myocardial enzyme assay results and routine blood tests after the treatment (Fig. 7c). The results of blood tests 2 hours before treatment were set as the baselines. All the biochemical results were analyzed by an automatic analyzer (ARCHITECT i2000sr, Abbott, Illinois 60064, USA).

Histopathological examination

The ablated livers were harvested at the above time points posttreatment. The liver vasculature was immediately flushed with 0.9% physiological saline solutions through the postcava for 5 minutes. After the saline perfusion, the ablated liver tissue was dissected and fixed with formalin for hematoxylin and eosin (H&E) staining.

Statistical analysis

The statistical blood biochemistry results, including liver function, myocardial enzyme assays and routine blood tests, were illustrated with column graphs using GraphPad Prism 8.0.1. The results for the nsPEF-treated and untreated groups were compared and analyzed with unpaired t-tests. The data are presented as the mean±SD. The statistical significance of p-value was demonstrated at $P^* < 0.05$, $P^{**} < 0.01$ and $P^{***} < 0.001$, ns: no significance.

Abbreviations

nsPEF: Nanosecond pulsed electric field; HCC: Hepatocellular carcinoma; IRE: Irreversible electroporation; RFA: Radiofrequency ablation; ECG: Electrocardiograph; TP: total protein; Alb: albumin; Glb: globulin; ALT: alanine aminotransferase; AST: aspartate aminotransferase; ALP: alkaline phosphatase; TB: total bilirubin; DB: direct bilirubin; TBA: total bile acid; CK: creatine kinase; CK-MB: creatine kinase isoenzyme; LDH: lactate dehydrogenase; HBDH: hydroxybutyrate dehydrogenase; RBC: red blood cell count; WBC: white blood cell count; NEUT: neutrophilic granulocyte percentage; Hgb: haemoglobin; HCT: haematocrit; PLT: blood platelet count; MCH: mean corpuscular haemoglobin; MCHC: mean corpuscular haemoglobin concentration; MCV: mean lcorpuscular volume; MWA: microwave ablation.

Declarations

Acknowledgements

All authors thank Professor Xinmei Chen from Shandong University of Traditional Chinese Medicine, who is currently a visiting scholar of Harvard University, USA, for kind proofreading; Liangjie Hong, Danjing Guo, and Haohao Lu for their technical assistance on animal experiments.

Authors' contributions

SSZ and WZ conceived and designed the experiments. JHL and JJQ performed the experiments and drafted the manuscript. SYZ, XHC, SYY and LZ participated in the experiments and analyzed the data. SSZ and WZ oversaw of all aspects of the study. All authors read and approved the manuscript.

Funding

This work was supported by the National S&T Major Project of China (No. 2018ZX10301201), the National Science Foundation of China (No.81721091, No. 2017ZX10203205).

Availability of data and materials

The datasets used and analyzed during the current study are available from the corresponding author on reasonable request.

Ethics approval and consent to participate

This study was approved by the Animal Care and Use Committee of Zhejiang University. The methods were carried out in accordance with the approved guidelines. All animals received appropriate humane care from certificated professional staff.

Consent for publication

Not applicable.

Competing interests

The authors declare that they have no competing interest.

Author details

[1] Division of Hepatobiliary and Pancreatic Surgery, Department of Surgery, First Affiliated Hospital, School of Medicine, Zhejiang University, Hangzhou 310003, China. [2] Key Laboratory of Combined Multi-organ Transplantation, Ministry of Public Health, Hangzhou 310002, China. [3] Key Laboratory of the Diagnosis and Treatment of Organ Transplantation, CAMS, Hangzhou 310002, China. [4] Collaborative Innovation Center for Diagnosis Treatment of Infectious Diseases, Zhejiang University, Hangzhou, China 310003. [5]

Shulan Hangzhou Hospital Affiliated to Zhejiang Shuren University Shulan International Medical College, Hangzhou 310006, China. [6] Zhejiang University School of Medicine, Hangzhou 310058, China.

References

1. Bray F, Ferlay J, Soerjomataram I, Siegel RL, Torre LA, Jemal A. Global cancer statistics 2018: GLOBOCAN estimates of incidence and mortality worldwide for 36 cancers in 185 countries. CA Cancer J Clin. 2018;68(6):394-424.
2. European Association for the Study of the Liver. Electronic address eee, European Association for the Study of the L. EASL Clinical Practice Guidelines: Management of hepatocellular carcinoma. J Hepatol. 2018;69(1):182-236.
3. Lu DS, Raman SS, Vodopich DJ, Wang M, Sayre J, Lassman C. Effect of vessel size on creation of hepatic radiofrequency lesions in pigs: assessment of the "heat sink" effect. AJR Am J Roentgenol. 2002;178(1):47-51.
4. Nishigaki Y, Tomita E, Hayashi H, Suzuki Y, Iritani S, Kato T, et al. Efficacy and safety of radiofrequency ablation for hepatocellular carcinoma in the caudate lobe of the liver. Hepatol Res. 2013;43(5):467-74.
5. Chiang J, Hynes K, Brace CL. Flow-dependent vascular heat transfer during microwave thermal ablation. Conf Proc IEEE Eng Med Biol Soc. 2012;2012:5582-5.
6. Sheiman RG, Mullan C, Ahmed M. In vivo determination of a modified heat capacity of small hepatocellular carcinomas prior to radiofrequency ablation: correlation with adjacent vasculature and tumour recurrence. Int J Hyperthermia. 2012;28(2):122-31.
7. Metcalfe MS, Mullin EJ, Texler M, Berry DP, Dennison AR, Maddern GJ. The safety and efficacy of radiofrequency and electrolytic ablation created adjacent to large hepatic veins in a porcine model. Eur J Surg Oncol. 2007;33(5):662-7.
8. Yoshimoto T, Kotoh K, Horikawa Y, Kohjima M, Morizono S, Yamashita S, et al. Decreased portal flow volume increases the area of necrosis caused by radio frequency ablation in pigs. Liver Int. 2007;27(3):368-72.
9. Livraghi T, Solbiati L, Meloni MF, Gazelle GS, Halpern EF, Goldberg SN. Treatment of focal liver tumors with percutaneous radio-frequency ablation: complications encountered in a multicenter study. Radiology. 2003;226(2):441-51.
10. Beebe SJ, White J, Blackmore PF, Deng Y, Somers K, Schoenbach KH. Diverse effects of nanosecond pulsed electric fields on cells and tissues. DNA Cell Biol. 2003;22(12):785-96.
11. Hall EH, Schoenbach KH, Beebe SJ. Nanosecond pulsed electric fields (nsPEF) induce direct electric field effects and biological effects on human colon carcinoma cells. DNA Cell Biol. 2005;24(5):283-91.
12. Frey W, White JA, Price RO, Blackmore PF, Joshi RP, Nuccitelli R, et al. Plasma membrane voltage changes during nanosecond pulsed electric field exposure. Biophys J. 2006;90(10):3608-15.

13. Beebe SJ, Fox PM, Rec LJ, Willis EL, Schoenbach KH. Nanosecond, high-intensity pulsed electric fields induce apoptosis in human cells. FASEB J. 2003;17(11):1493-5.
14. Pakhomov AG, Shevin R, White JA, Kolb JF, Pakhomova ON, Joshi RP, et al. Membrane permeabilization and cell damage by ultrashort electric field shocks. Arch Biochem Biophys. 2007;465(1):109-18.
15. Gao C, Zhang X, Chen J, Zhao J, Liu Y, Zhang J, et al. Utilizing the nanosecond pulse technique to improve antigen intracellular delivery and presentation to treat tongue squamous cell carcinoma. Med Oral Patol Oral Cir Bucal. 2018;23(3):e344-e50.
16. Nuccitelli R, Wood R, Kreis M, Athos B, Huynh J, Lui K, et al. First-in-human trial of nanoelectroablation therapy for basal cell carcinoma: proof of method. Exp Dermatol. 2014;23(2):135-7.
17. Pliquett U, Nuccitelli R. Measurement and simulation of Joule heating during treatment of B-16 melanoma tumors in mice with nanosecond pulsed electric fields. Bioelectrochemistry. 2014;100:62-8.
18. Beebe SJ, Lassiter BP, Guo S. Nanopulse Stimulation (NPS) Induces Tumor Ablation and Immunity in Orthotopic 4T1 Mouse Breast Cancer: A Review. Cancers (Basel). 2018;10(4).
19. Miao X, Yin S, Shao Z, Zhang Y, Chen X. Nanosecond pulsed electric field inhibits proliferation and induces apoptosis in human osteosarcoma. J Orthop Surg Res. 2015;10:104.
20. Guo S, Burcus NI, Hornef J, Jing Y, Jiang C, Heller R, et al. Nano-Pulse Stimulation for the Treatment of Pancreatic Cancer and the Changes in Immune Profile. Cancers (Basel). 2018;10(7).
21. Lassiter BP, Guo S, Beebe SJ. Nano-Pulse Stimulation Ablates Orthotopic Rat Hepatocellular Carcinoma and Induces Innate and Adaptive Memory Immune Mechanisms that Prevent Recurrence. Cancers (Basel). 2018;10(3).
22. Bismuth H, Majno PE. Hepatobiliary surgery. J Hepatol. 2000;32(1 Suppl):208-24.
23. Fan WJ, Wu PH, Zhang L, Huang JH, Zhang FJ, Gu YK, et al. Radiofrequency ablation as a treatment for hilar cholangiocarcinoma. World J Gastroenterol. 2008;14(28):4540-5.
24. Zervas NT, Kuwayama A. Pathological characteristics of experimental thermal lesions. Comparison of induction heating and radiofrequency electrocoagulation. J Neurosurg. 1972;37(4):418-22.
25. Yin S, Chen X, Hu C, Zhang X, Hu Z, Yu J, et al. Nanosecond pulsed electric field (nsPEF) treatment for hepatocellular carcinoma: a novel locoregional ablation decreasing lung metastasis. Cancer Lett. 2014;346(2):285-91.
26. Vogl TJ, Straub R, Eichler K, Woitaschek D, Mack MG. Malignant liver tumors treated with MR imaging-guided laser-induced thermotherapy: experience with complications in 899 patients (2,520 lesions). Radiology. 2002;225(2):367-77.
27. Raman SS, Aziz D, Chang X, Ye M, Sayre J, Lassman C, et al. Minimizing central bile duct injury during radiofrequency ablation: use of intraductal chilled saline perfusion--initial observations from a study in pigs. Radiology. 2004;232(1):154-9.

28. Nagata Y, Hiraoka M, Nishimura Y, Masunaga S, Mitumori M, Okuno Y, et al. Clinical results of radiofrequency hyperthermia for malignant liver tumors. Int J Radiat Oncol Biol Phys. 1997;38(2):359-65.
29. Lee DS, Dorian P, Downar E, Burns M, Yeo EL, Gold WL, et al. Thrombogenicity of radiofrequency ablation procedures: what factors influence thrombin generation? Europace. 2001;3(3):195-200.
30. Aras KK, Efimov IR. Irreversible electroporation: Proceed with caution. Heart Rhythm. 2018;15(12):1880-1.
31. Deodhar A, Dickfeld T, Single GW, Hamilton WC, Jr., Thornton RH, Sofocleous CT, et al. Irreversible electroporation near the heart: ventricular arrhythmias can be prevented with ECG synchronization. AJR Am J Roentgenol. 2011;196(3):W330-5.
32. Kostrzewa M, Tueluemen E, Rudic B, Rathmann N, Akin I, Henzler T, et al. Cardiac impact of R-wave triggered irreversible electroporation therapy. Heart Rhythm. 2018;15(12):1872-9.
33. Golberg A, Rubinsky B. Towards electroporation based treatment planning considering electric field induced muscle contractions. Technol Cancer Res Treat. 2012;11(2):189-201.
34. Yao C, Dong S, Zhao Y, Lv Y, Liu H, Gong L, et al. Bipolar Microsecond Pulses and Insulated Needle Electrodes for Reducing Muscle Contractions During Irreversible Electroporation. IEEE Trans Biomed Eng. 2017;64(12):2924-37.
35. Castellvi Q, Mercadal B, Moll X, Fondevila D, Andaluz A, Ivorra A. Avoiding neuromuscular stimulation in liver irreversible electroporation using radiofrequency electric fields. Phys Med Biol. 2018;63(3):035027.

Table

monitoring of tissue impedance and electric current during the ablation.

ctric current (A)	Impedance (Ω)	Duration time of single pulse (ns)	Pulse numbers	Needle distance (cm)
116	215.52	300	800	1
112	223.21	300	800	1
116	215.52	300	800	1
115	217.39	300	800	1
119	210.08	300	800	1
117	213.68	300	800	1
115	217.39	300	800	1
113	221.24	300	800	1
108	231.48	300	800	1.2
103	242.72	300	800	1.3
101	247.52	300	800	1.5
96	260.42	300	800	2

Supplementary File Legend

Additional file 1: Table S1. Results of cardiac troponin I (ng/ml).

Figures

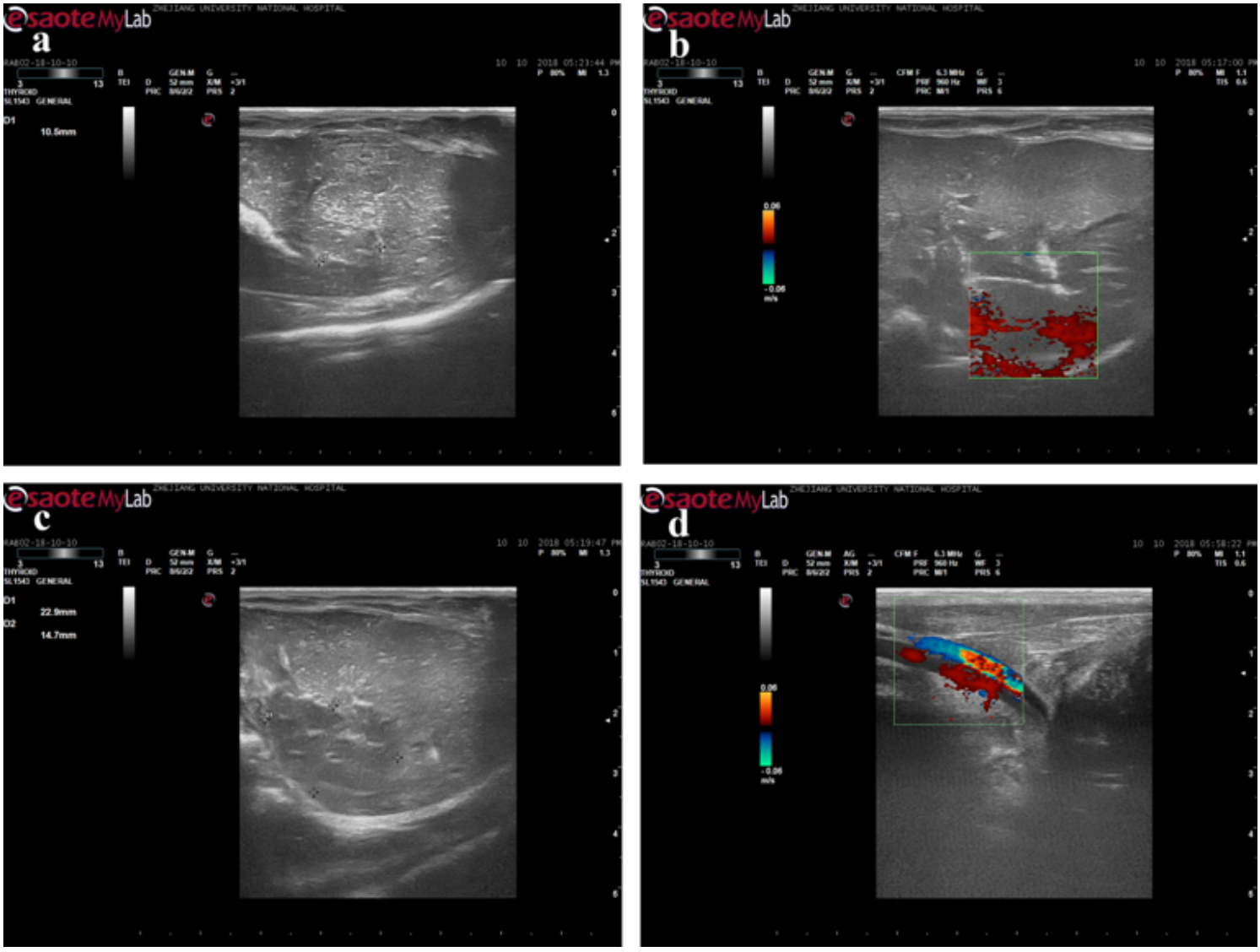

Figure 1

Real time monitoring by ultrasonography during nsPEF treatment. (a) The distance between the two needles under ultrasonic guidance was 10.5 mm. (b) Ultrasonography confirmed that there was no puncture-related vessel damage. (c) The ultrasonography image demonstrated a 14.7 mm * 22.9 mm hypoechoic area 15 minutes after the ablation. (d) The blood flow situation was observed after the treatment.

Figure 2

Pathological specimen from the nsPEF-treated liver tissues. The upper and lower groups of the figures represent the unfixed and formalin-fixed liver tissues at 2 hours, 2 days, 7 days, 14 days and 28 days posttreatment, respectively. At 14 days posttreatment, there was a clear demarcation line between the

treated area and normal liver tissue. Congestion and swelling were obvious in the treated area but had partially resolved at approximately 7 days posttreatment. At 14 days posttreatment, some of the treated area became fibrotic and gradually wrapped with omentum. By day 28, the congestion was almost resolved and the ablated area showed conglutination with the peritoneum. The vessels and biliary systems seen traversing the area appeared intact.

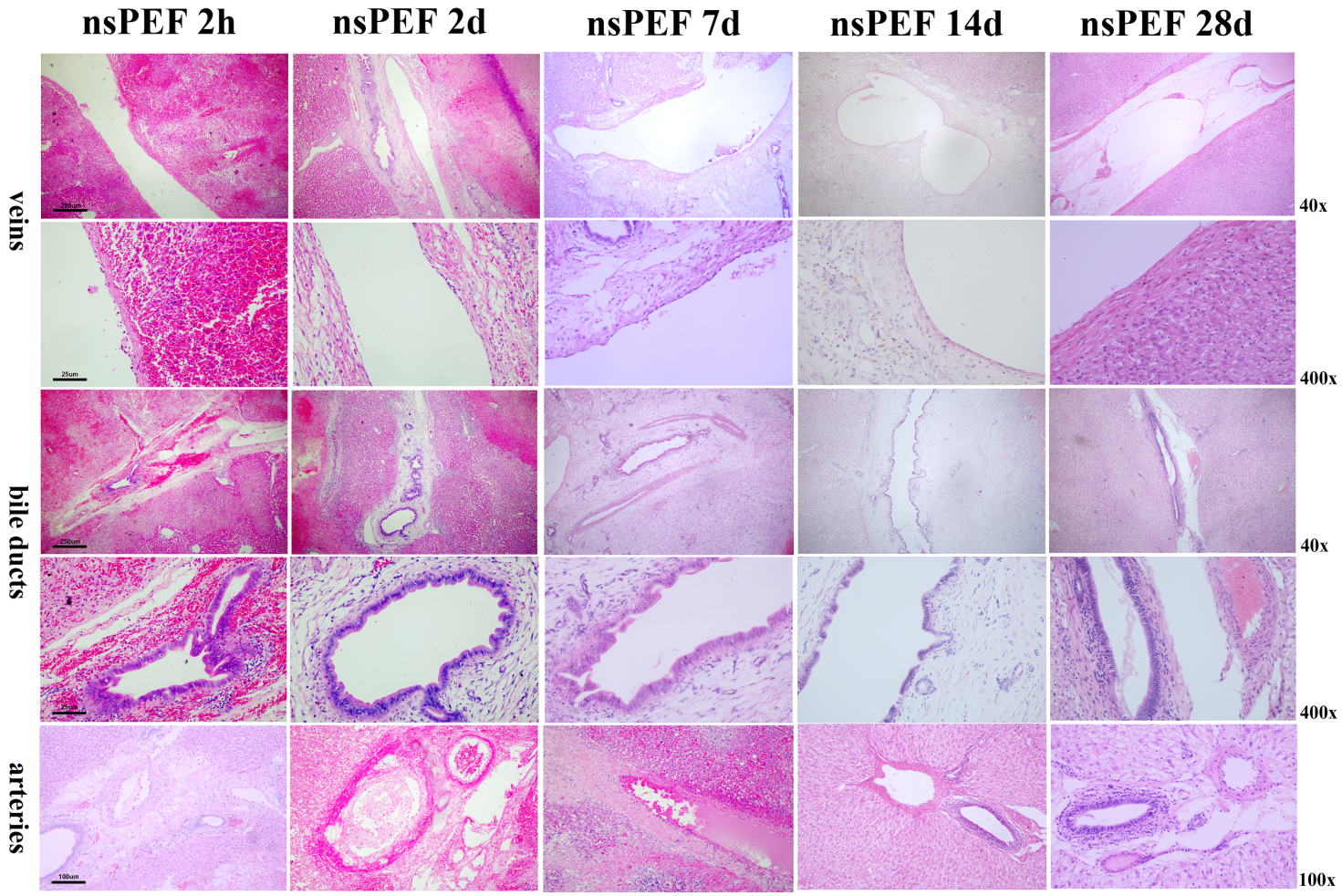

Figure 3

Haematoxylin and eosin (H&E) stained sections. Figure 3 shows the different hepatic vasculatures after the ablation in time order, including hepatic veins and bile ducts. At 2 hours posttreatment, the hepatic sinusoids were infiltrated with massive amounts of red blood cells. Most of the large vessels maintained a complete structure and the endothelial layer remained intact, while parts of the endothelial layers had been shed from the vessel wall. The bile ducts in the ablated area showed no acute damage. By 2 days posttreatment, some of the microveins in the ablated area had been destroyed, and the large vessels, though structurally preserved, demonstrated partial endothelial loss, neutrophil infiltration, and mild vasculitis. The bile ducts in the ablation zone showed mild signs of edema but no necrosis. Extensive infiltration of red blood cells, granulocytes and other inflammatory cells infiltrated was observed in the sinusoids. On the 7th day, the inflammation had resolved in most of the area and the damaged endothelia of the large vessels began the process of reendothelialization. Some of the neovasculature appeared around the large vessels and the margin of the ablated area. From the 14 days to 28 days

posttreatment, the dead hepatocytes were gradually replaced by fibroblast tissues. Hepatocellular regeneration appeared in most of the ablated area. Scale bars were presented in the first picture of each row: 250μm for 40× and 25μm for 400× under microscope.

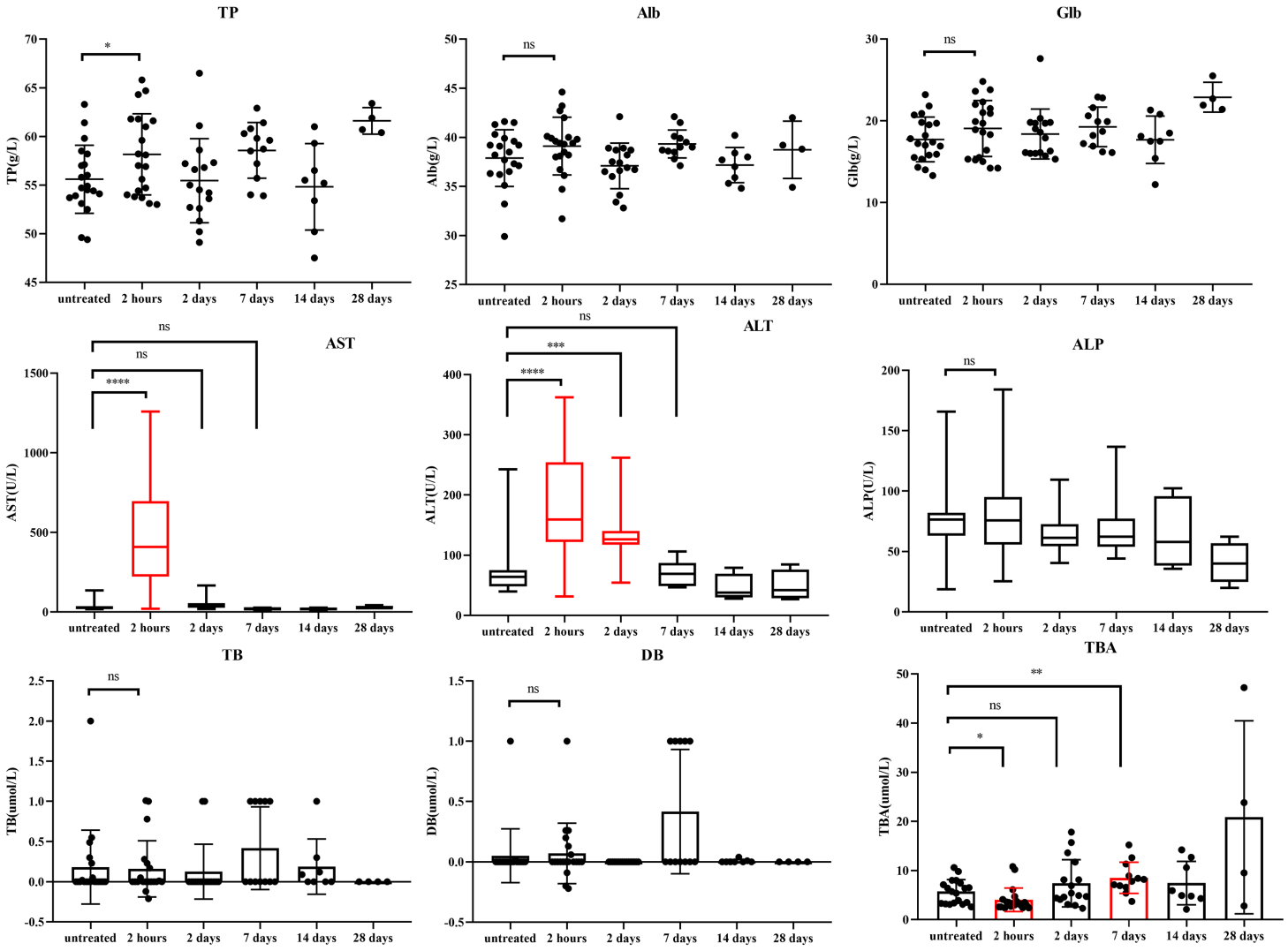

Figure 4

Liver function follow-up. Liver function results for each rabbit at 2 hours, 2 days, 7 days, 14 days and 28 days posttreatment were compared with the pretreatment results, illustrating a mild disturbance of liver function posttreatment and a subsequent recovery. The tested liver function results included total protein (TP), albumin (Alb), globulin (Glb), alanine aminotransferase (ALT), aspartate aminotransferase (AST), alkaline phosphatase (ALP), total bilirubin (TB), direct bilirubin (DB) and total bile acid (TBA). Blood samples were collected pretreatment and 2 hours, 2 days, 7 days, 14 days and 28 days posttreatment. Data are presented as the mean±sd. P* < 0.05, P** < 0.01, P *** < 0.001, ns: no significance.

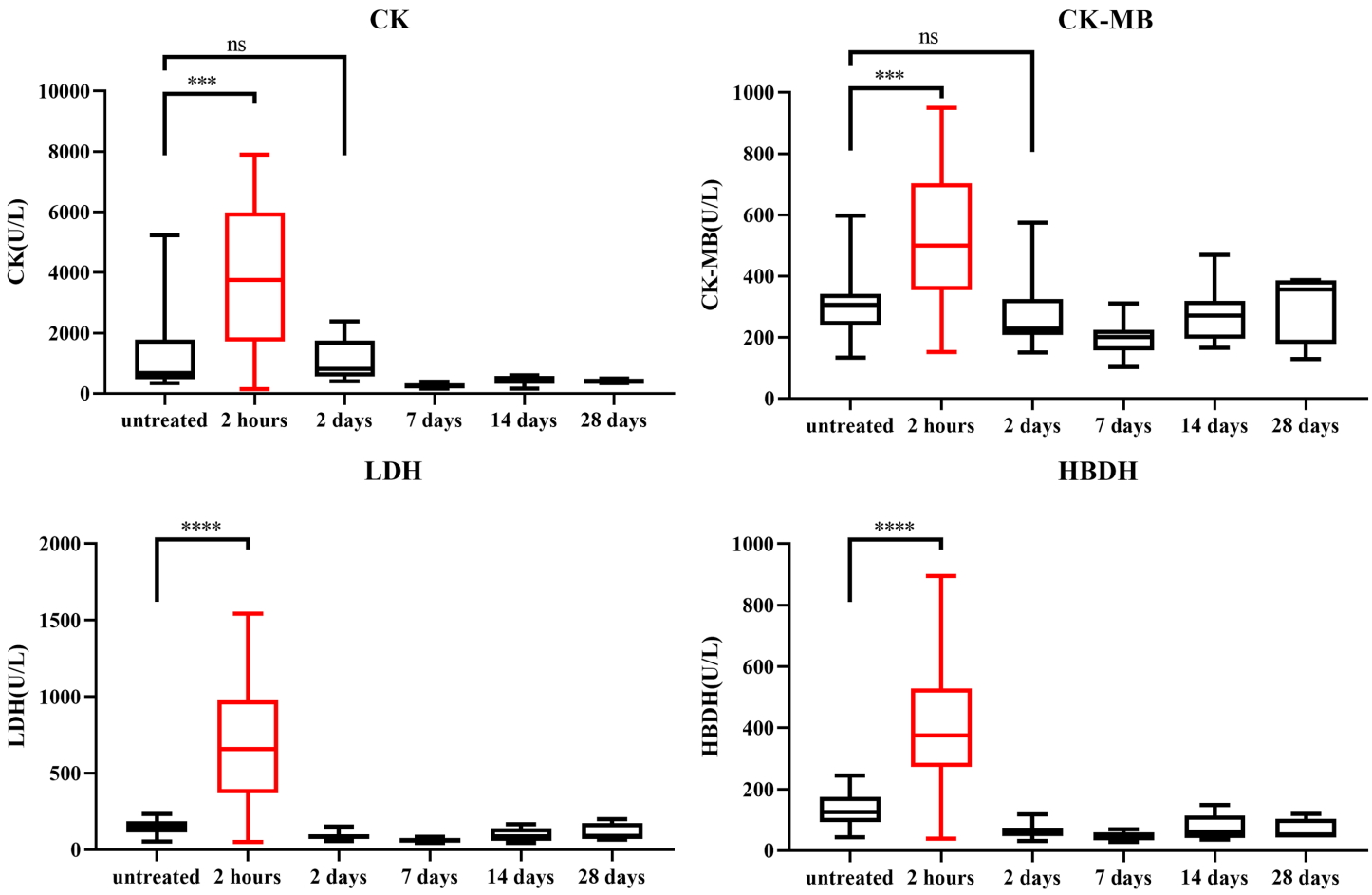

Figure 5

Myocardial enzymogram at follow-up. Myocardial enzyme assay results for each rabbit at 2 hours, 2 days, 7 days, 14 days and 28 days posttreatment were compared with those of the untreated counterparts in time order, which demonstrated transient stimulation-induced damage of myocardial enzymes and self-recovery processes without sequelae. The myocardial enzyme assay indexes included heart type creatine kinase (CK), creatine kinase isoenzyme (CK-MB), lactate dehydrogenase (LDH), and hydroxybutyrate dehydrogenase (HBDH). Blood samples were collected pretreatment and 2 hours, 2 days, 7 days, 14 days and 28 days posttreatment. Data are presented as the mean±sd. P* < 0.05, P** < 0.01, P *** < 0.001, ns: no significance.

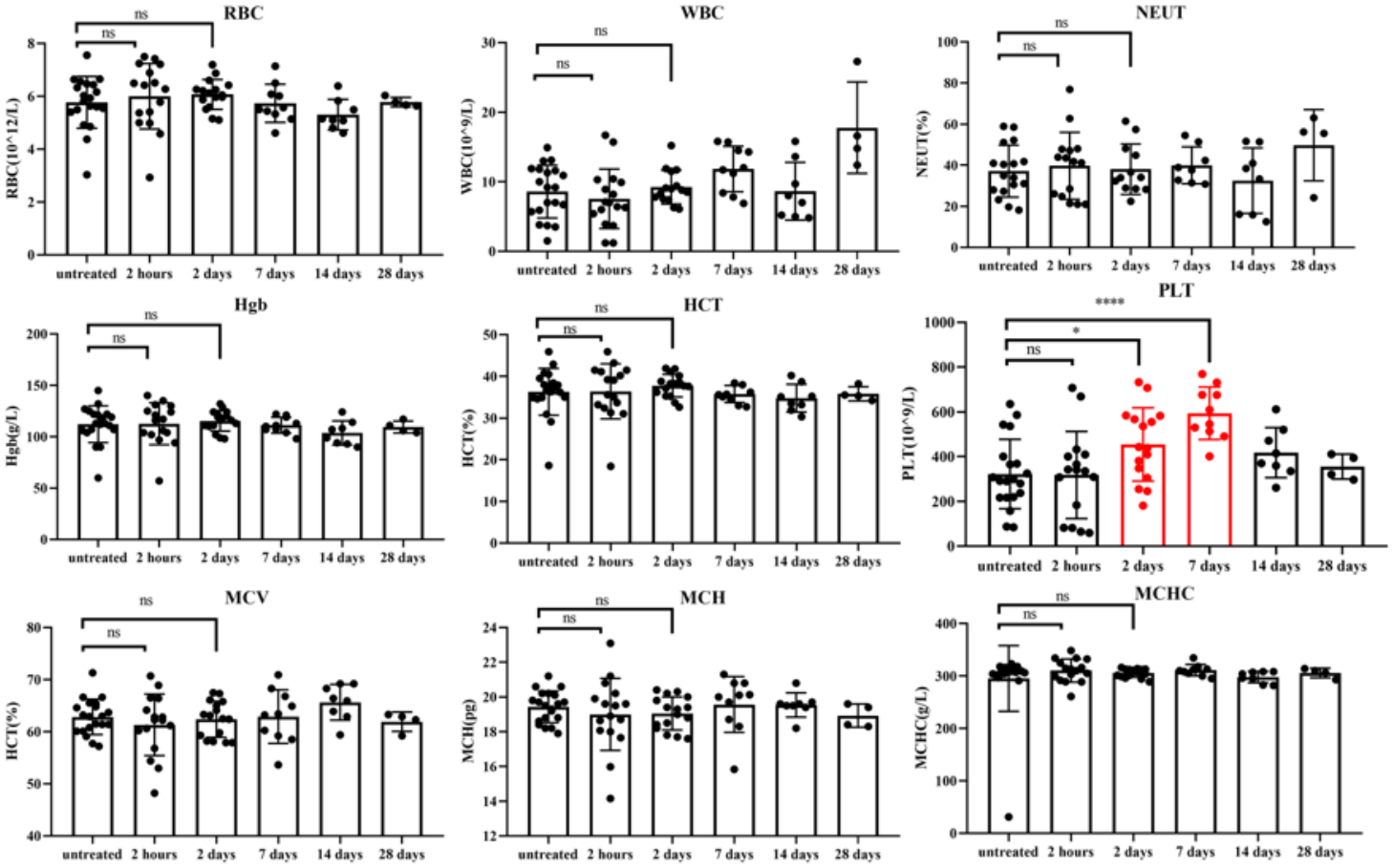

Figure 6

Routine blood test at follow-up. Routine blood test results for each rabbit at 2 hours, 2 days, 7 days, 14 days and 28 days posttreatment were compared with those for untreated counterparts in time order, which showed no obvious changes and indicated a controlled risk of infection during the treatment. The routine blood test results included the red blood cell count (RBC), white blood cell count (WBC), neutrophilic granulocyte percentage (NEUT), hemoglobin (Hb), hematocrit (HCT), blood platelet count (PLT), mean corpuscular hemoglobin (MCH), and mean corpuscular hemoglobin concentration (MCHC), and mean corpuscular volume (MCV). Blood samples were collected pretreatment and 2 hours, 2 days, 7 days, 14 days, and 28 days posttreatment. Data are presented as the mean±sd. P* < 0.05, P** < 0.01, P *** < 0.001, ns: no significance.

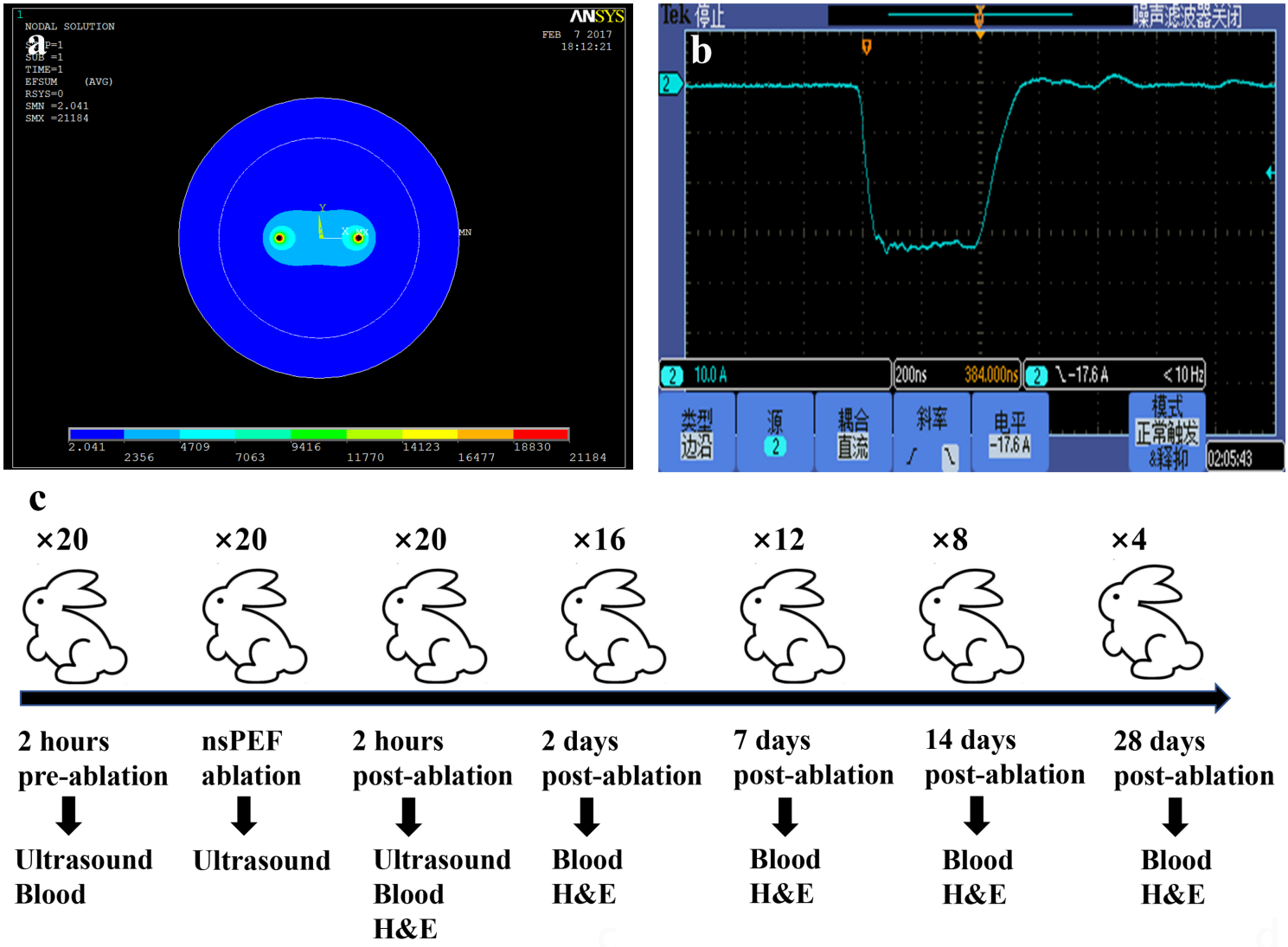

Figure 7

Schematic diagram of nsPEF and the animal experimental design. (a) The ablation area and its according temperature were pre-calculated by software simulation according to the distance between the two electrodes. (b) The pulse shape was monitored during the procedure. (c) A total of 20 rabbits underwent nsPEF ablation. Four rabbits were euthanized at 2 hours, 2 days, 7 days, 14 days and 28 days posttreatment. Blood samples and liver tissues were obtained at each of the time points.

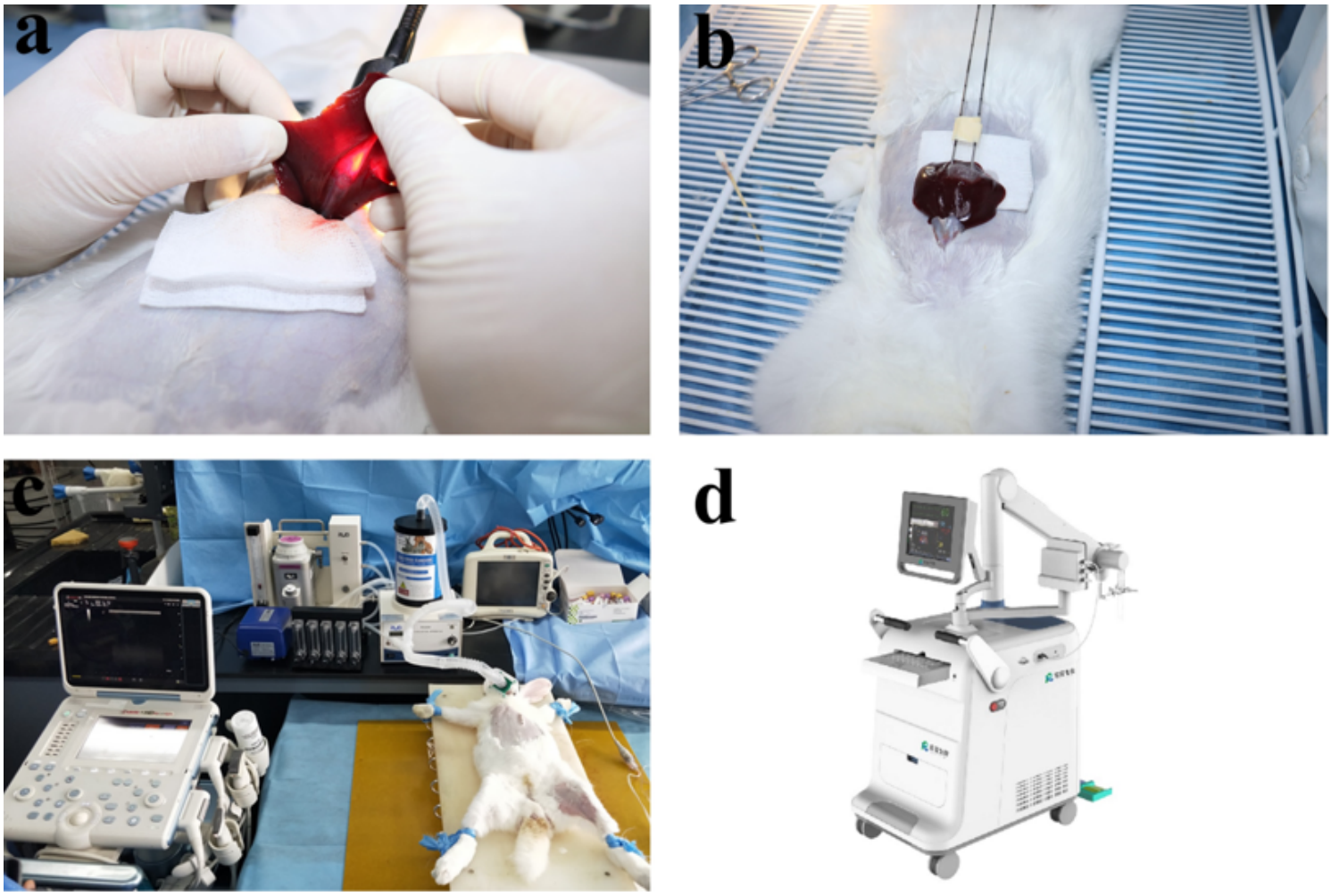

Figure 8

Nanosecond pulsed electric field treatment settings. (a) The treatment was performed via open laparotomy to directly identify the location of the porta hepatis where the bile ducts and large vessels converged. (b) The two-needle electrode was inserted into the identified location with a tip depth of approximately 2 cm. (c) General anesthesia was maintained with mechanical ventilation. (d) The nsPEF prototype used in this experiment.

Supplementary Files

This is a list of supplementary files associated with this preprint. Click to download.

- Additionalfile1.xlsx